

# FPGA BASED MAXIMUM POWER POINT TRACKING OF PHOTOVOLTAIC SYSTEM

KING DIAW A/L EH SUT

A project report submitted in partial  
fulfillment of the requirement for the award of the  
Master of Electrical Engineering

Faculty of Electrical and Electronic Engineering  
Universiti Tun Hussein Onn Malaysia

JANUARY 2014

## **ABSTRACT**

Nowadays, PV cell which is known as a photovoltaic is one of the most important parts in electrical field to convert photo light to voltage and current at the desired output voltage and frequency by using varies control techniques. This project presents design and implementation of FPGA Based Maximum Power Point Tracking (MPPT) Controller for Photovoltaic system. The MPPT controller is employed to control and get Maximum Power Point (MPP) from the source. Altera DE1 board devices are used as a controller for the implementation of the MPPT system. The simulation of this FPGA based MPPT controller is designed and implemented using Quartus II VHDL software tools. The results shown, the same signal obtained from Matlab simulink software as compared with Quartus II. It has been observed that the designed system has been successfully extracting the MPP from the pseudo sources used in the simulations. The system has been evaluated in sunny day and partially shaded conditions to analyze the respective outputs in these conditions.

## CONTENTS

	<b>TITLE</b>	<b>i</b>
	<b>DECLARATION</b>	<b>ii</b>
	<b>DEDICATION</b>	<b>iii</b>
	<b>ACKNOWLEDGEMENT</b>	<b>iv</b>
	<b>ABSTRACT</b>	<b>v</b>
	<b>CONTENTS</b>	<b>vi</b>
	<b>LIST OF TABLE</b>	<b>ix</b>
	<b>LIST OF FIGURE</b>	<b>x</b>
	<b>LIST OF SYMBOLS AND ABBREVIATIONS</b>	<b>xiii</b>
	<b>LIST OF APPENDICES</b>	<b>xiv</b>
<b>CHAPTER 1</b>	<b>INTRODUCTION</b>	<b>1</b>
	1.1 Project Background	1
	1.2 Problem Statement	3
	1.3 Project Objectives	3
	1.4 Scope Project	3
<b>CHAPTER 2</b>	<b>LITERATURE REVIEW</b>	<b>5</b>
	2.1 Introduction	5
	2.2 Photovoltaic (PV) Generation	5
	2.2.1 Photovoltaic Model	7
	2.3 Maximum Power Point Tracking (MPPT)	8
	2.4 MPPT from the dc-dc converter point of view	10

2.5	MPPT from the tracking algorithm point of view	12
2.5.1	Perturb and Observe	12
2.5.2	Constant Conductance	14
2.6	Field Programmable Gate Array (FPGA)	15
2.6.1	FPGA Architectures	15
2.6.2	ALTERA Technology	16
2.6.3	Altera DE1 board	16
2.7	VHDL Programming	18
2.8	Design Entry Using VHDL and Schematic Capture	18
<b>CHAPTER 3</b>	<b>METHODOLOGY</b>	20
3.1	Introduction	20
3.2	Flow Chart	20
3.3	Project Development using MATLAB-Simulink	21
3.3.1	Photovoltaic Modeling	22
3.3.2	Verifying PV Module Modeling	28
3.3.3	MPPT Algorithm	33
3.3.4	Verify P&O Model in MATLAB-Simulink	35
3.4	Developing MPPT using Quartus II	36
3.4.1	P&O Method implement by Quartus II Software	37
3.4.2	Verify P&O Model in Quartus II software	39
3.4.3	Downloading ALTERA DE1 board	40
<b>CHAPTER 4</b>	<b>RESULT AND ANALYSIS</b>	43
4.1	Introduction	43
4.2	Verification result of MPPT model	43
4.3	MPPT model simulate using Simulink	45
4.3.1	Input graph for PV module	45
4.3.2	Analysis of MPPT parameters.	46

4.4	MPPT model simulate using Quartus II software	52
<b>CHAPTER 5</b>	<b>CONCLUSION AND RECOMMENDATION</b>	56
5.1	Conclusion	56
5.2	Recommendations	57
	<b>REFERENCES</b>	58
	<b>APPENDIX</b>	61

**LIST OF TABLE**

<b>NO</b>	<b>TITLE</b>	<b>PAGE</b>
Table 2.1	Electrical Characteristic of MSX-60	8
Table 2.2	FPGA Technologies type and companies	15
Table 3.1	Electrical Characteristics of MSX-60	30
Table 3.2	Testing Condition	31
Table 3.3	Variation of reference voltage according to the variations in power and voltage output	39
Table 3.4	Control logic of MUX	39
Table 3.5	Dummy input Voltage and Current	40

## LIST OF FIGURE

<b>NO</b>	<b>TITLE</b>	<b>PAGE</b>
Figure 2.1	I-V curve from Kyocera KC200GT PV module: (a) under constant temperature and (b) under constant irradiance.	6
Figure 2.2	P-V curve from Kyocera KC200GT PV module obtained by simulation: (a) under constant temperature and (b) under constant solar radiation.	6
Figure 2.3	Identification of $I_{sc}$ , $V_{oc}$ , $I_{mpp}$ , $V_{mpp}$ and $P_{mpp}$ on the I-V and P-V curves.	7
Figure 2.4	The single-diode model of a practical photovoltaic device.	7
Figure 2.5	MPP across the I-V plan considering solar radiation and temperature changes.	9
Figure 2.6	Typical input and output data related to MPPT algorithms.	9
Figure 2.7	PV module supplying a resistive load.	10
Figure 2.8	Definition of the system operating point by the I-V and load curves intersection.	11
Figure 2.9	I-V and load curves intersection for defining the PV system operating point.	11
Figure 2.10	Maximum point tracker system	12
Figure 2.11	Flow chart of P&O algorithm	13
Figure 2.12	Incremental conductance algorithm [11]	14
Figure 2.13	Altera DE1 board	17
Figure 2.14	Implementation of block symbol file	19
Figure 3.1	Flow chart of project development	21
Figure 3.2	Equivalent circuit of a single solar cell	23
Figure 3.3	Flow of calculating the output current of a PV module	26

Figure 3.4	PV module model in MATLAB-Simulink. (a) Block diagram of the PV module model. (b) PV module in a subsystem	27
Figure 3.5	Screen shot of Embedded MATLAB Editor	28
Figure 3.6	Verifying method	31
Figure 3.7	(a) I-V curve obtain from simulation, (b) I-V curve provide by manufacturer	32
Figure 3.8	P&O model in MATLAB-Simulink. (a) Block diagram of the P&O model. (b) P&O model in a subsystem	34
Figure 3.9	Screen shot of Embedded MATLAB Editor	35
Figure 3.10	Screen Shot Model Explorer of Subsystem MPPT-P&O	35
Figure 3.11	Simulation schematic of boost topology to verify P&O algorithm	36
Figure 3.13	(a) Block diagram of P&O Method (b) implemented in Quartus II Software	38
Figure 3.14	verification result	40
Figure 3.15	screen shot of modification input side	41
Figure 3.16	Pin planner assign in Quartus II software	41
Figure 3.17	Downloading process of Mppt development on Quartus II software	42
Figure 4.1	Result of simulation in the case of uniform irradiance	44
Figure 4.2	Result of simulation in the case of nonuniform irradiance	44
Figure 4.3	Input irradiance for PV module	45
Figure 4.4	Input cell temperature for PV module	46
Figure 4.5	Configuration on input irradiance and temperature in simulation	46
Figure 4.6	Case 1 - MPPT output power from MATLAB-Simulink	47
Figure 4.7	Case 1 - (a) Overview MPPT output voltage reference ( $V_{ref}$ ), (b) zoom-in view of $V_{ref}$ from MATLAB-Simulink	48
Figure 4.8	Case 1 - Photovoltaic current from MATLAB-Simulink	49
Figure 4.9	Case 1 - (a) Overview value of duty cycle (b) zoom-in value of duty cycle from MATLAB-Simulink.	50
Figure 4.10	Case 2 - MPPT output power from MATLAB-Simulink	50

Figure 4.11	Case 2 - MPPT output voltage reference ( $V_{ref}$ ), from MATLAB-Simulink	51
Figure 4.12	Case 2 - Photovoltaic current from MATLAB-Simulink	51
Figure 4.13	Case 2 - (a) Overview value of duty cycle (b) zoom-in value of duty cycle from MATLAB-Simulink.	52
Figure 4.14	(a) Input voltage and current for case 1, (b) input voltage and current for case 2	53
Figure 4.15	Screen shot of output vector waveform file	54
Figure 4.16	Comparison of duty signal (a) case 1, (b) case 2	55

**LIST OF SYMBOLS AND ABBREVIATIONS**

$I_{ph}$  - Photocurrent;

$I_d$  - Current of parallel diode;

$I_{sh}$  - Shunt current;

$I$  - Output current;

$V$  - Output voltage;

$D$  - Parallel diode;

$R_{sh}$  - Shunt resistance;

$R_s$  - Series resistance;

**LIST OF APPENDICES**

<b>APPENDIX</b>	<b>TITLE</b>	<b>PAGE</b>
A	Complete S-Function Program	61
B	Embedded VHDL code of each block diagram	62
C	Input voltage and current	67
D	MPPT Controller in Block Diagram File (.bdf)	74

## **CHAPTER 1**

### **INTRODUCTION**

#### **1.1 Project Background**

Photovoltaic (PV) offers an environmentally friendly source of electricity since it is clean, pollution free and inexhaustible. However, the output from a PV solar cell alone is not good enough to input into an electricity bank or in to the main grid because its output is not constant in terms of voltage. This raises a need to design a controller which can calculate and extract the maximum power point (MPP) at any instant from the solar cells.

Maximum Power Point Tracking, frequently referred as MPPT, is an electronic system that operates the Photovoltaic (PV) modules in a manner that allow the modules to produce all the power they are capable of on that time. MPPT is not a mechanical tracking system that “physically moves” the module to make them point more directly at the sun but it is a fully electronic system that varies the electrical operating point of the module so that modules are able to deliver maximum available power. To understand how MPPT works, refer to section 2.3.

The researches on the MPPT area are normally grouped in two categories: the first one relates to the dc-dc converter topology optimization, focusing on methods to determine a suitable dc-dc converter for operating as MPPT [1]; and the second one refers to the maximum power point tracking algorithm, used to control the dc-dc converter in order to establish the system operating point as close as possible to the Maximum Power Point (MPP) [2]. Therefore, an efficient MPPT system needs to be

composed by the integration of an adequate dc-dc converter (hardware) and proper tracking algorithm (software).

By looking at the MPPT tracking algorithm point of view there are various methods of MPPT. These methods are implemented by designing various algorithms like Perturb-and-observe (P&O) method, Open- and Short-circuit method, Incremental Conductance algorithm, and other algorithms. The best MPPT technique base on cost versus energy generation is the P&O [2]. Since accuracy and fast tracking response conflict one from other, the mentioned tracking methods cannot satisfy, simultaneously, both of them. In place of the traditional and spread methods, some researcher have proposed complex MPPT algorithms, based on fuzzy logic and neural network, in order to accomplish fast tracking response and accuracy in a single system. These proposals, however, present some disadvantageous: needed for high processing capacity, increasing the complexity and cost of the design, in some cases, employment of extra sensors.

To implement the purpose MPPT algorithm, there are many technologies that available now days. The following is a commonly used controller; Microcontroller base implementation [3], [4], Digital Signal Processing (DSP) base implementation [5], and FPGA base implementation [6].

Field Programmable Gate Array (FPGA) based systems provide a number of runtime advantages over the sequential machines such as a microcontroller. In addition, concurrent operations may be executed continuously and simultaneously faster than Digital Signal Processing (DSP) device. Since the functions of various components can be integrated onto the same chip, FPGAs offer lower implementation cost than DSPs that can perform only DSP-related computations. Moreover, FPGAs can provide equivalent or higher performance with the customization potential of an ASIC, it is useful to processing the complex algorithm that implement artificial intelligent (AI). As FPGAs can also be reprogrammed at any time, this ability can also provide a high level of flexibility: the MPPT control system can be easily updated or modified even when it is running [7].

While by looking at the MPPT dc-dc converter point of view, there are many types of dc-dc converter has been proposed such Buck and Boost converter. However, based on observation done by Coelho [8] obtain Boost converter has higher energy efficiency than Buck converter.

## 1.2 Problem Statement

Photovoltaic (PV) system has become an important source of power for a wide range of applications. Unfortunately, PV generation systems have two major problems: the conversion efficiency of electric power generation is very low (9-17%) [2], especially under low irradiation conditions and the amount of electric power generated by solar arrays change continuously with weather conditions. Moreover, the solar cell V-I characteristic is nonlinear and varies with irradiation and temperature. In general, there is a unique point on the V-I or V-P curve, called the Maximum Power Point (MPP), at which the entire PV system operates with maximum efficiency and produces its maximum output power. The location of the MPP is not known, but can be located, either through calculation models or by search algorithm. Therefore, Maximum Power Point Tracking (MPPT) techniques are needed to maintain the PV array's operating point at its MPP.

## 1.3 Project Objectives

The primary objective of this project is to develop the FPGA based MPPT controller of photovoltaic system.

In addition, this project has various objectives, which comprise of:

- i. To design the optimum controller by simulation for the maximum power point tracking.
- ii. To analyze simulations result of the maximum power point controller tracking.
- iii. To implement maximum power point controller on FPGA board.

## 1.4 Scope Project

The scope of this project is limit to:

- i. The MPPT algorithm applied FPGA base, responsible for properly controlling the dc-dc converter in order to establish the system operating point as close as possible to the Maximum Power Point (MPP).

- ii. Use Block Diagram/Schematic and VHDL program to put the algorithm into FPGA and simulate the MPPT controller using Quartus II software.
- iii. Use MATLAB-SIMULINK to verify the result.

## **CHAPTER 2**

### **LITERATURE REVIEW**

#### **2.1 Introduction**

This chapter is about the discussion of all the summarized information of the relevant studies to implement FPGA on designing the MPPT method for PV system. The Quartus II software implemented using Block Diagram/Schematic and VHDL programming for Field Programmable Gate Array (FPGA) and the features of Altera DE1 board. Furthermore, this chapter is also discussing about a study on the previous research based on journals and conferences. The sources of the literatures review are from journals, conferences and books.

#### **2.2 Photovoltaic (PV) Generation**

Photovoltaic modules output power depends on two factors which is cell temperature and solar irradiation, resulting in a non-linear and time-variant power source.

The cell temperature and solar radiation are strongly coupled, the temperature mainly influences the PV module output voltage, while the solar radiation mostly influences the PV module output current, as depicts the I-V curve presented at Figure 2.1, obtained from Kyocera KC200GT PV module datasheet.

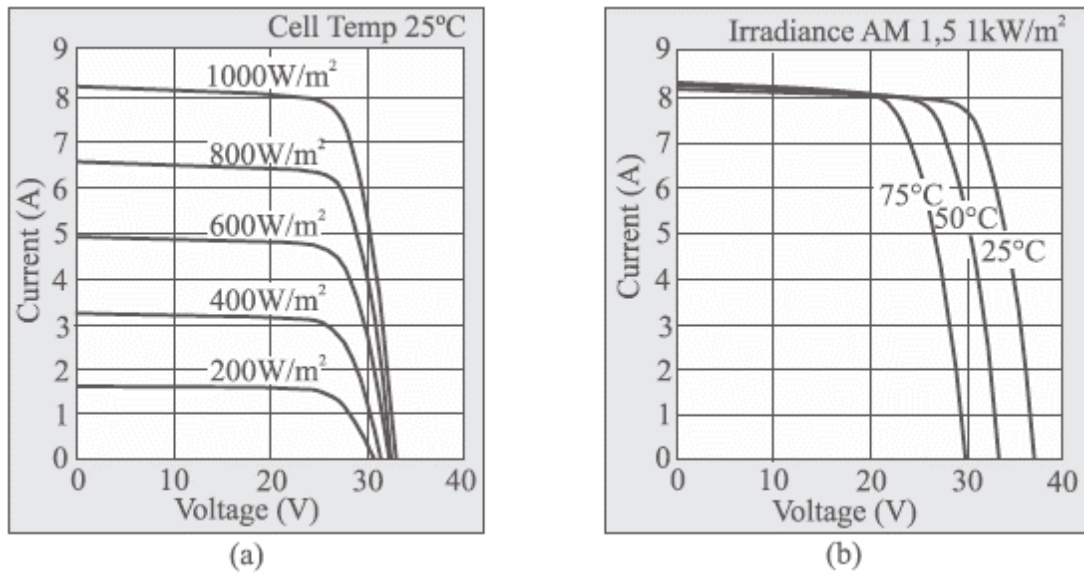


Figure 2.1: I-V curve from Kyocera KC200GT PV module: (a) under constant temperature and (b) under constant irradiance.

One of most important PV module operation point is obtained on the knee of the I-V curve. In this point, named by maximum power point (MPP), the product of the PV output voltage and current results at the maximum available power, for a given solar radiation and temperature. For emphasizing the maximum power point, an alternative P-V (power versus voltage) curve may be plotted, in accordance with Figure 2.2

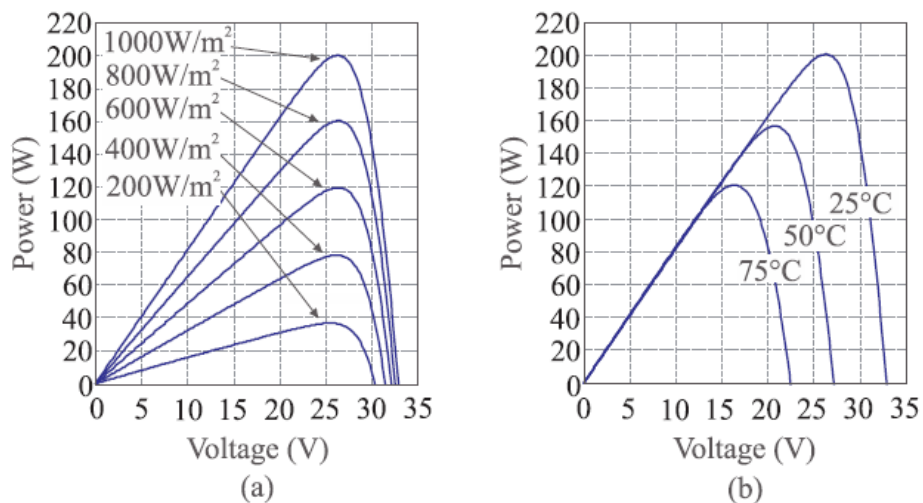


Figure 2.2: P-V curve from Kyocera KC200GT PV module obtained by simulation: (a) under constant temperature and (b) under constant solar radiation.

Furthermore, short circuit current ( $I_{sc}$ ) and open circuit voltage ( $V_{oc}$ ) are also important for a complete PV module characterization. They represent the points where the PV generated power is zero, but the output current or voltage reach the maximum value, respectively. Figure 2.3 highlights  $I_{sc}$ ,  $V_{oc}$ ,  $I_{mpp}$ ,  $V_{mpp}$  and  $P_{mpp}$  on both, I-V and P-V curves.

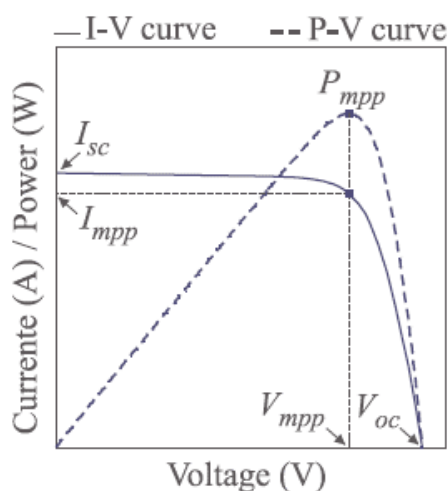


Figure 2.3: Identification of  $I_{sc}$ ,  $V_{oc}$ ,  $I_{mpp}$ ,  $V_{mpp}$  and  $P_{mpp}$  on the I-V and P-V curves.

### 2.2.1 Photovoltaic Model

To model solar cell, the one-diode model has been proposed [9], and some researchers have studied how to extract parameters for the model [9], [10]. Figure 2.4 shows the single-diode model.

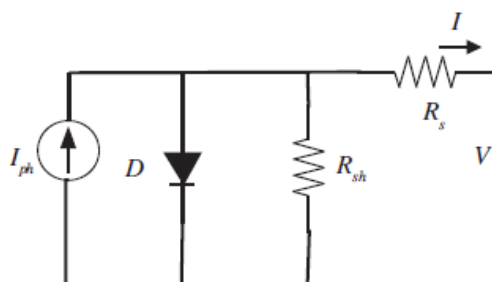


Figure 2.4: The single-diode model of a practical photovoltaic device.

In this project, a PV module, MSX-60, produced by Solarex's Megamodule™ series is chosen. In the next chapter, the mathematical modeling will be deriving

according to single-diode model and parameter from MSX-60 module. The electrical characteristic of MSX-60 is described in Table 2.1.

Table 2.1: Electrical Characteristic of MSX-60

<i>Typical Electrical Characteristics</i>	<i>MSX-60</i>
Maximum power (Pmax)	60W
Voltage @ Pmax (Vmp)	17.1V
Current @ Pmax (Imp)	3.5A
Guaranteed minimum Pmax	58W
Short-circuit current (Isc)	3.8A
Open-circuit voltage (Voc)	21.1V
Temperature coefficient of open-circuit voltage	$-(80 \pm 10)mV/^{\circ}C$
Temperature coefficient of short-circuit current	$(0.065 \pm 0.015)\%/^{\circ}C$
Temperature coefficient of power	$-(0.5 \pm 0.05)\%/^{\circ}C$
NOCT <sup>2</sup>	$47 \pm 2^{\circ}C$

### 2.3 Maximum Power Point Tracking (MPPT)

For maximizing the PV conversion efficiency, the incoming sun energy must be converted to electricity with the highest efficiency, accomplished when the photovoltaic module operates on the maximum power point [8]. However, since this operating point is mainly affected by the solar radiation and temperature levels, it may randomly vary along the I-V plan, as illustrates Figure 2.5.

Thus, in order to dynamically set the MPP as operation point for a wide range of solar radiation and temperature, specific circuits, known at the literature by Maximum Power Point Trackers (MPPT), are employed.

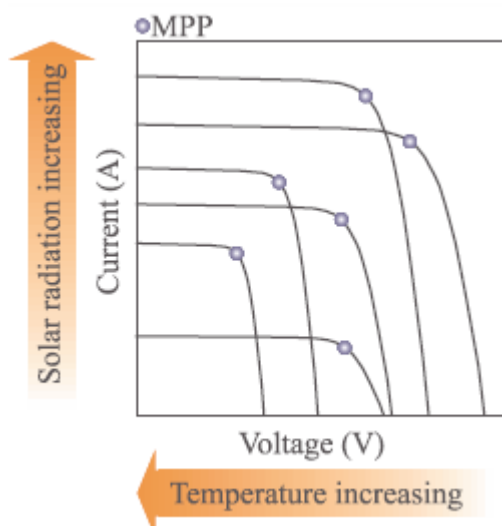


Figure 2.5: MPP across the I-V plan considering solar radiation and temperature changes.

In most applications, the MPPT is a simple dc-to-dc converter placed between the photovoltaic modules and the load, and its control is achieved through a tracking algorithm as illustrated in Figure 2.6.

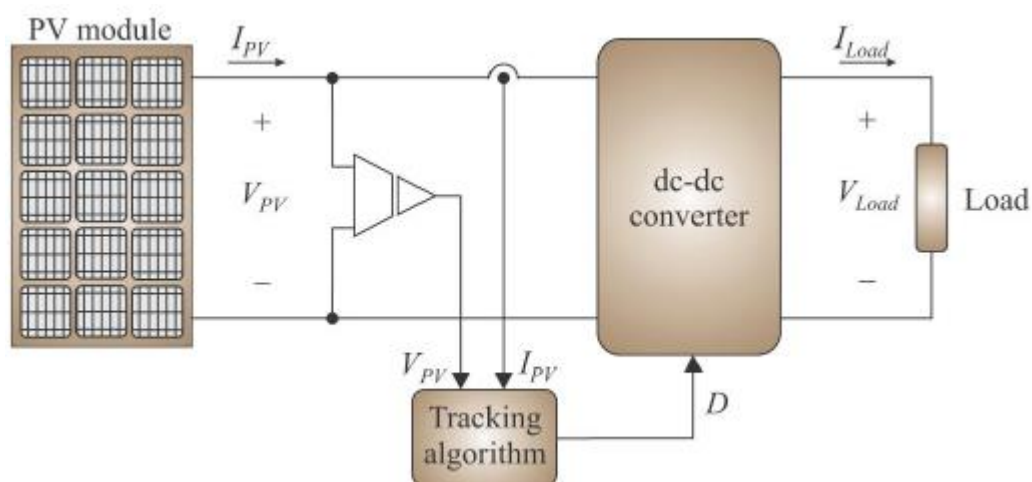


Figure 2.6: Typical input and output data related to MPPT algorithms.

The researches on the MPPT area are normally grouped in two categories: the first one relates to the dc-to-dc converter topology optimization, focusing on methods to determine a suitable dc-to-dc converter for operating as MPPT [1]; and the second one refers to the maximum power point tracking algorithm, responsible for properly

controlling the dc-to-dc converter in order to establish the system operating point as close as possible to the Maximum Power Point (MPP).

Therefore, an efficient MPPT system need to be composed by the integration of an adequate dc-to-dc converter (hardware) and proper tracking algorithm (software), resulting in some desired aspects:

- i. Fast tracking response (dynamic analysis);
- ii. Accuracy and no oscillation around the MPP (steady-state analysis);
- iii. Capacity to track the MPP for wide ranges of solar radiation and temperature;
- iv. Simplicity of implementation;
- v. Low cost.

#### 2.4 MPPT from the dc-to-dc converter point of view

The operating point of a photovoltaic system is defined by the I-V generation and load curves intersection. For more understanding how it occurs, firstly consider a PV module supplying a resistive load, as depicts Figure 2.7.

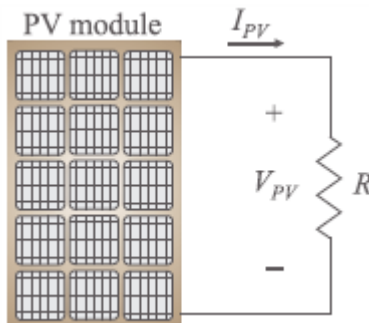


Figure 2.7: PV module supplying a resistive load.

The load curve is accomplished by the Ohm's Law while the generation curve is related to the PV I-V curve. Both curves are represented at Figure 2.8. Even when the load resistance is chosen for both curves intercept each other exactly on the MPP, it is impossible to ensure the maximum power transfer for long time intervals [8], once when solar radiation or temperature change, the MPP is relocated on the I-V plan.

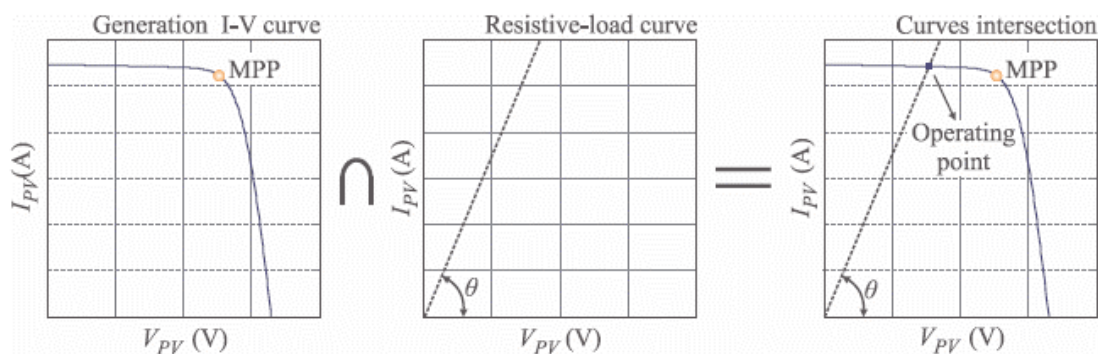


Figure 2.8: Definition of the system operating point by the I-V and load curves intersection.

For solving this problem, in order to maintain the system always operating on the MPP, the load curve should be modified according to solar radiation or temperature changes. For example, from Figure 2.9, if the PV generation curve is  $I-V$  1 and the load curve is  $Load$  1, the operating point is given by  $MPP$  1. Next, considering a solar radiation and temperature change, the generation curve comes from  $I-V$  1 to  $I-V$  2. In this situation, keeping the same load curve ( $Load$  1), the operating point is established at  $X2$ , i.e., out of the MPP. Nevertheless, if the load curve is modified from  $Load$  1 to  $Load$  2, the system backs to operate on the MPP, in this case,  $MPP$  2.

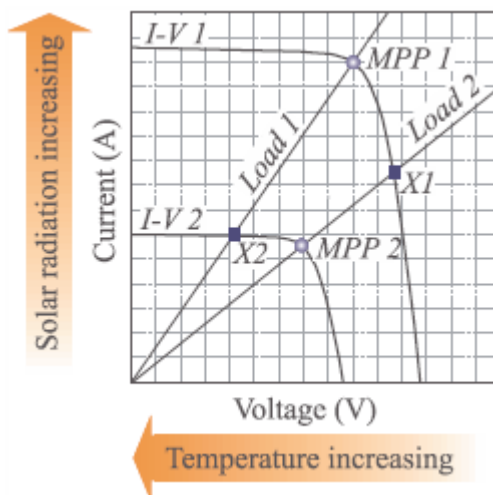


Figure 2.9: I-V and load curves intersection for defining the PV system operating point.

Evidently, modifying the load curve in accordance with the solar radiation and temperature changes is not an appropriate solution, since the load is defined by

the user. However, if a dc-to-dc converter is placed between the PV module and the load, it is possible to control the converter duty cycle in order to change a variable load from the PV terminals point of view, even when a fixed load is employed. The arrangement presented at Figure 2.10, composed by a PV module, a dc-to-dc converter and a load, defines the hardware of a maximum power point tracking system.

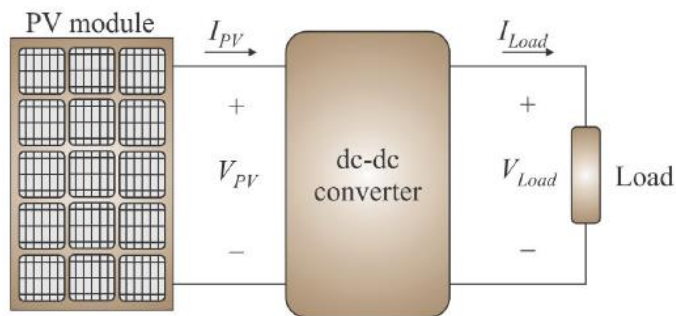


Figure 2.10: Maximum point tracker system

As conclusion, the Maximum Power Transfer in solar photovoltaic applications is achieved by impedance matching with a dc-to-dc converter.

## 2.5 MPPT from the tracking algorithm point of view

MPPT so far has 7 methods which are (i) Constant Voltage, (ii) Open Circuit Voltage, (iii) Short Circuit Current, (iv) Perturb and Observe, (v) Incremental Conductance, (vi) Temperature and (iiiv) Temperature Parametric. All the MPPT algorithms are designed to dynamically extract the maximum power from the PV panels. One of the more complete analyses of MPPT methods is given in [2]. Among these techniques, the P&O and the incremental conductance algorithms are the most popular due to its simplicity and the number of research paper has been published. Thus, in this section will be focus on describing on these two methods only.

### 2.5.1 Perturb and Observe

The concept behind the "perturb and observe" (P&O) method is to modify the operating voltage or current of the photovoltaic panel until obtain the maximum power from it. For example, if increasing the voltage to a panel increases the power

output of the panel, the system continues increasing the operating voltage until the power output begins to decrease. Once this happens, the voltage is decreased to get back towards the maximum power point. This perturbation continues indefinitely. Therefore, the power output value oscillates around a maximum power point and never stabilizes [8].

Figure 2.11 shows the flow chart of P&O method where (k) is current state of value, (k-1) is previous state value, and C is step size. After one perturbs operation the current power is calculated and compared with previous value to determine the change of power  $\Delta P$ . If  $\Delta P > 0$ , then the operation continues in the same direction of perturbation. Otherwise the operation reverses the perturbation direction.

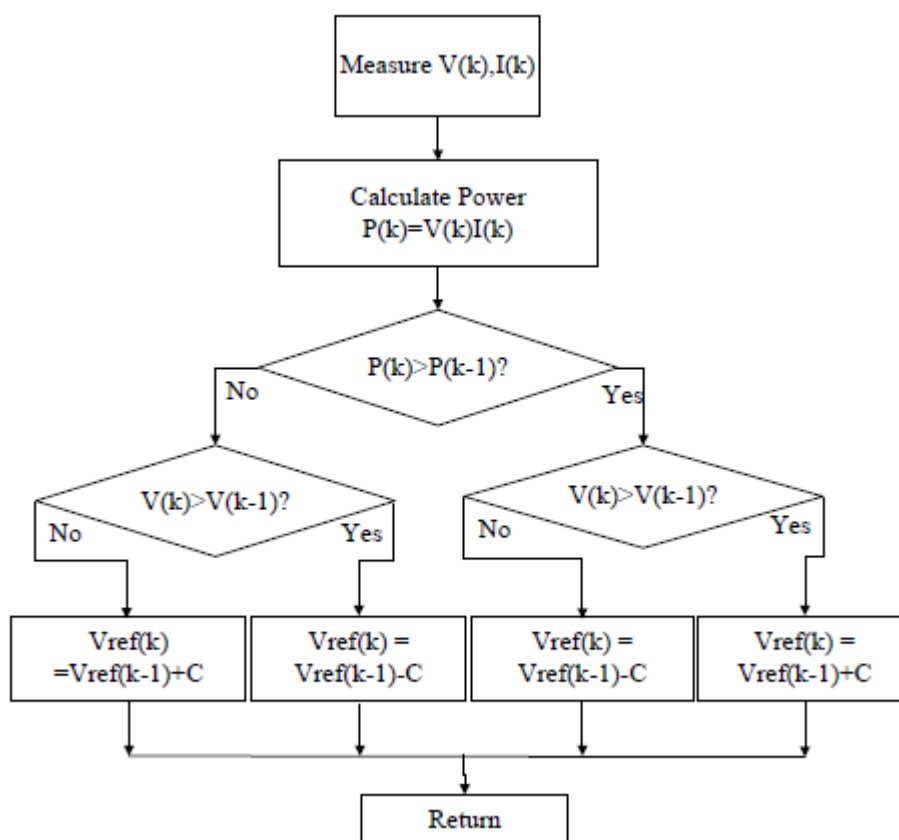


Figure 2.11: Flow chart of P&O algorithm

### 2.5.2 Constant Conductance

Constant conductance considers the fact that the slope of the power-voltage curve is zero at the maximum power point, positive at the left of the MPP, and negative at the right of the MPP. The MPP is found by comparing the instantaneous conductance ( $I/V$ ) to the incremental conductance ( $\Delta I/\Delta V$ ) [11]. This algorithm is based on the principle that at the MPP  $\partial p/\partial v=0$ , and as  $P = IV$  it yields

$$\begin{cases} \partial P/\partial V = 0 & \text{at } V = V_{mpp} \\ \partial P/\partial V > 0 & \text{at } V < V_{mpp} \\ \partial P/\partial V < 0 & \text{at } V > V_{mpp} \end{cases}$$

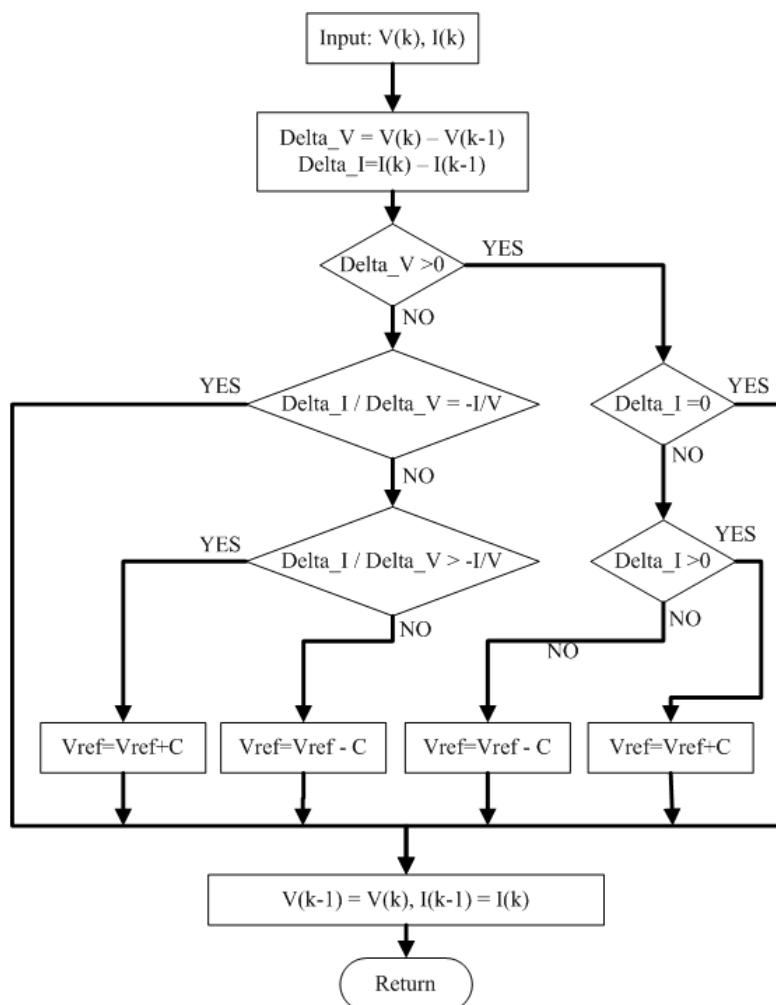


Figure 2.12: Incremental conductance algorithm [11]

This technique is characterized for presenting high tracking speed (variable step) and accuracy (no oscillation), however, it is more complex than P&O, once the derivative must be calculated in real time and also require a voltage and a current sensor.

## 2.6 Field Programmable Gate Array (FPGA)

A Field-Programmable Gate Array (FPGA) is an integrated circuit designed to be configured by the customer or designer after manufacturing. FPGA are programmed using a logic circuit diagram or a source code in a Hardware Description Language (HDL) to specify how the chip will operate. Previously, the Application-Specific Integrated Circuit (ASIC) in circuit diagrams form is used to specify the configuration. A combination of volume, fabrication improvements, research and development, and the I/O capabilities of new supercomputers have largely closed the performance gap between ASICs and FPGAs.

FPGAs originally began as competitors to CPLDs (Complex Programmable Logic Device). As their size, capabilities, and speed increased, FPGAs began to take over larger and larger functions to the state where some are now marketed as full Systems on Chips (SoC). Applications of FPGAs include digital signal processing, software-defined radio, aerospace and defense systems, ASIC prototyping, medical imaging, computer vision, speech recognition, cryptography, bioinformatics, computer hardware emulation, radio astronomy, metal detection and a growing range of other areas. FPGAs are increasingly used in conventional high performance computing applications where computational kernels such as FFT or Convolution are performed on the FPGA instead of a microprocessor.

### 2.6.1 FPGA Architectures

Table 2.2: FPGA Technologies type and companies

Company	Low-cost FPGA	High density FPGA	FPGA with embedded processors, DSP and transceivers	FPGA with More DSP and LUT6	Latest
Altera	Cyclone	Stratix	Stratix GX,	Stratix IV,	Stratix V

			Excalibur	Cyclone III	Cyclone V
Xilinx	Spartan	Virtex	Virtex II Pro, Virtex 4, Virtex5 (LUT6)	Virtex 6, Spartan 6	Virtex 7, Kintex 7, Artix7

### 2.6.2 ALTERA Technology

Altera Corporation is a Silicon Valley manufacturer of PLDs, reconfigurable complex digital circuits. The company released its first PLD in 1984. Altera's main products are the Stratix, Arria and Cyclone series FPGAs, the MAX series CPLDs (Complex programmable logic devices), the HardCopy series ASICs and Quartus II design software.

The Stratix and Cyclone series FPGAs are the company's largest, highest bandwidth devices, with up to 1.1 million logic elements, integrated transceivers at up to 28 Gbit/s, up to 1.6 Tbit/s of serial switching capability, up to 1,840 GMACs of signal processing performance, and up to 7 x72 DDR3 memory interfaces at 800 MHz.

Cyclone series FPGAs and SoC FPGAs are the company's lowest cost, lowest power FPGAs, with variants offering integrated transceivers up to 5 Gbit/s. In between these two device families are Arria series FPGAs and SoC FPGAs, which provide a balance of performance, power, and cost for mid-range applications such as remote radio heads, video conferencing equipment, and wire line access equipment.

### 2.6.3 Altera DE1 board

The Altera DE1 board has many features that allow the user to implement a wide range of designed circuits, from simple circuits to various multimedia projects. A photograph of the DE1 board is shown in Figure 2.13. It depicts the layout of the board and indicates the location of the connectors and key components. In order to use the DE1 board, the user has to be familiar with the Quartus II software.

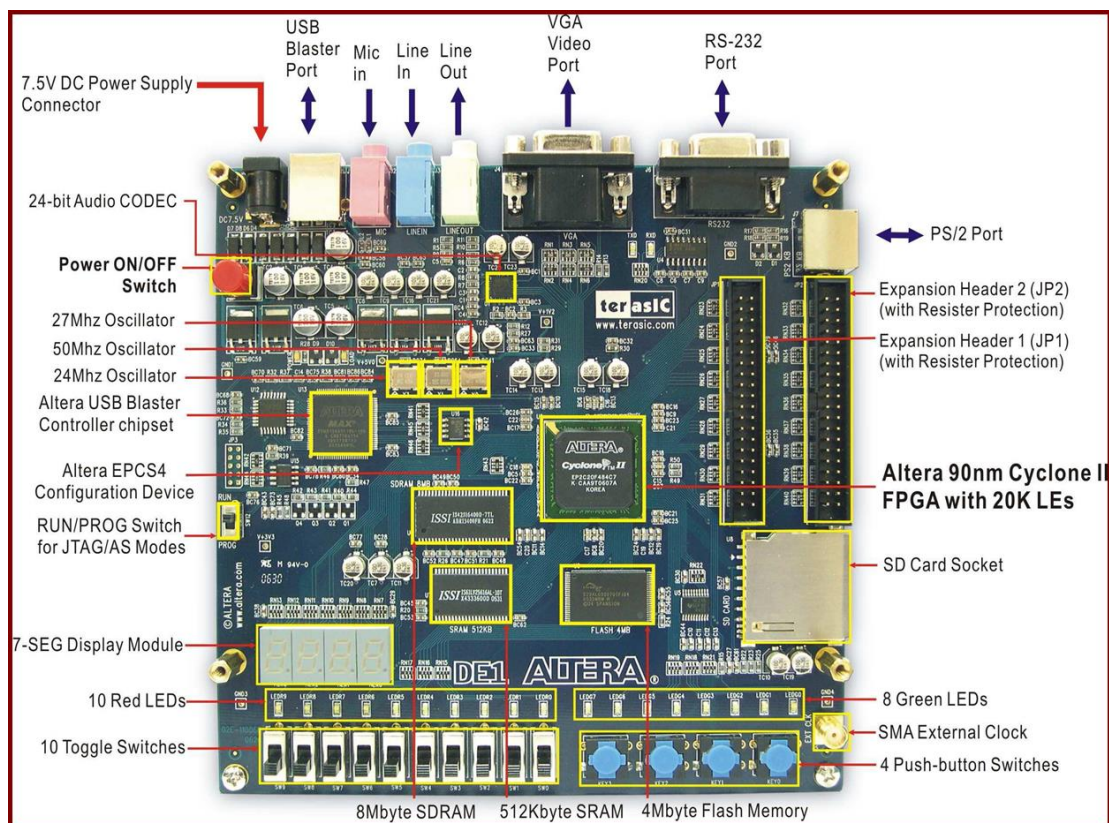


Figure 2.13: Altera DE1 board

Some of the hardware provided on the Altera DE1 board is:

- i. Cyclone II EP2C20F484C7 FPGA and EPCS4 serial configuration device
- ii. Built-in USB Blaster for FPGA configuration RS-232 port
- iii. VGA DAC resistor network (4096 colors)
- iv. PS/2 mouse or keyboard port
- v. Line-in, Line-out, microphone-in (24-bit audio CODEC).
- vi. Expansion headers (76 signal pins)
- vii. 8-MB SDRAM, 512-KB SRAM, 4-MB Flash
- viii. SD memory card slot
- ix. 10 toggle switches
- x. 4 debounced pushbutton switches
- xi. 10 red LEDs, 8 green LEDs
- xii. Four 7-segment displays
- xiii. 27-MHz and 50-MHz oscillators, external SMA clock input

## 2.7 VHDL Programming

VHDL stands for VHSIC Hardware description Language. VHSIC means Very High Speed Integrated Circuit. VHDL is a hardware description language which describes the behavior of an electronic circuit or system from which the physical circuit or system can be attained or implemented. This hardware description language has become popular nowadays in the electronics design community due to its ability to easily migrate code from one system to another. Since a VHDL design is just a text file, it can be used with a wide variety of software tools without worrying about data compatibility. VHDL is a computer language used to model and synthesize digital hardware. As its title implies, VHDL is used to describe the structure or behavior of hardware, and then determine how it should operate (modeling) or how it should be built (synthesis).

A programmer enters text according to the syntax of language, then use appropriate software to compile, simulate and synthesize the design. In this project, the Quartus II software is will be used as a compiler and simulator.

After the design process using VHDL is done, the simulation part of the waveform will be simulate using Vector Waveform File (.vwf). By using the waveform editor, the .vwf can be easily viewed and edited.

## 2.8 Design Entry Using VHDL and Schematic Capture

Apart of producing a design just using VHDL or Schematic capture User also can create a project that mixing VHDL and schematic capture by using mixture of design-entry methods

The VHDL code representing the block function is written in the Quartus II Text Editor. The Quartus II also can be used to compile the VHDL code. When the compilation is finished and no error, that code can be convert into block symbol file. The “Create/Update” command used to create a Block Symbol File (.bsf) from a VHDL design file, and then incorporate it into a Block Design File (.bdf).

A symbol file has been created can be uses in schematic capture as a function block as illustrated in Figure 2.14

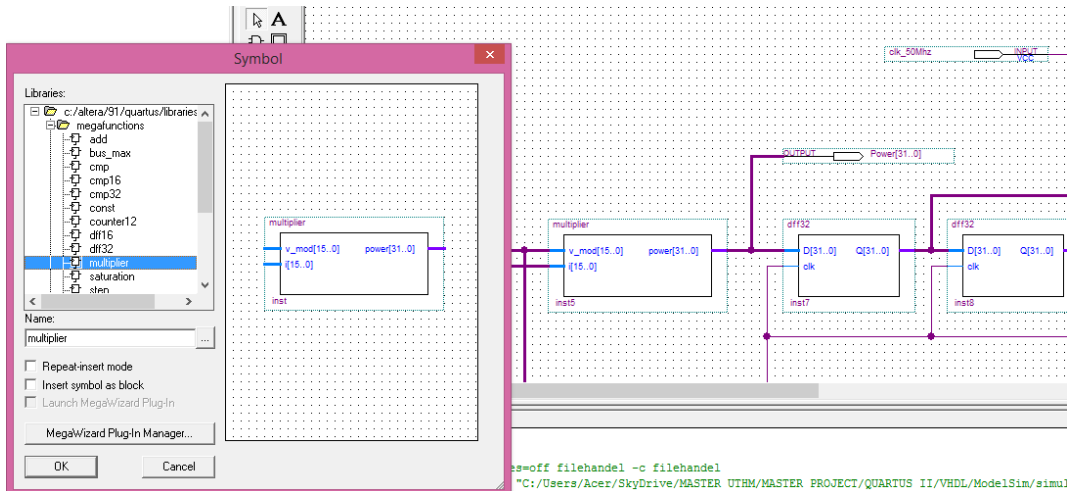


Figure 2.14: Implementation of block symbol file

## **CHAPTER 3**

### **METHODOLOGY**

#### **3.1 Introduction**

This chapter will discuss about the method that have been used to develop the project including the tool, equipment, procedure and processes involved in the hardware and software development and implementation of the project. The methodology process utilizes both software simulation and hardware construction. It is virtual to simulate the system by using software to get the theoretical result before hardware designation can be made.

#### **3.2 Flow Chart**

The primary tools for develop this project is Matlab/Simulink software package. This project has divided into two phases. In the first stage, the development of solar module and design controller for the MPPT PV system is built. After simulation circuit part, the next stage is the programming of PV system using VHDL from the data obtained on Matlab using Quartus II software. Lastly, the programming developed is downloaded into Altera DE1 board and interfaced with the PV system. The output of the PV system is analyzed in MPPT output current, voltage, and power.

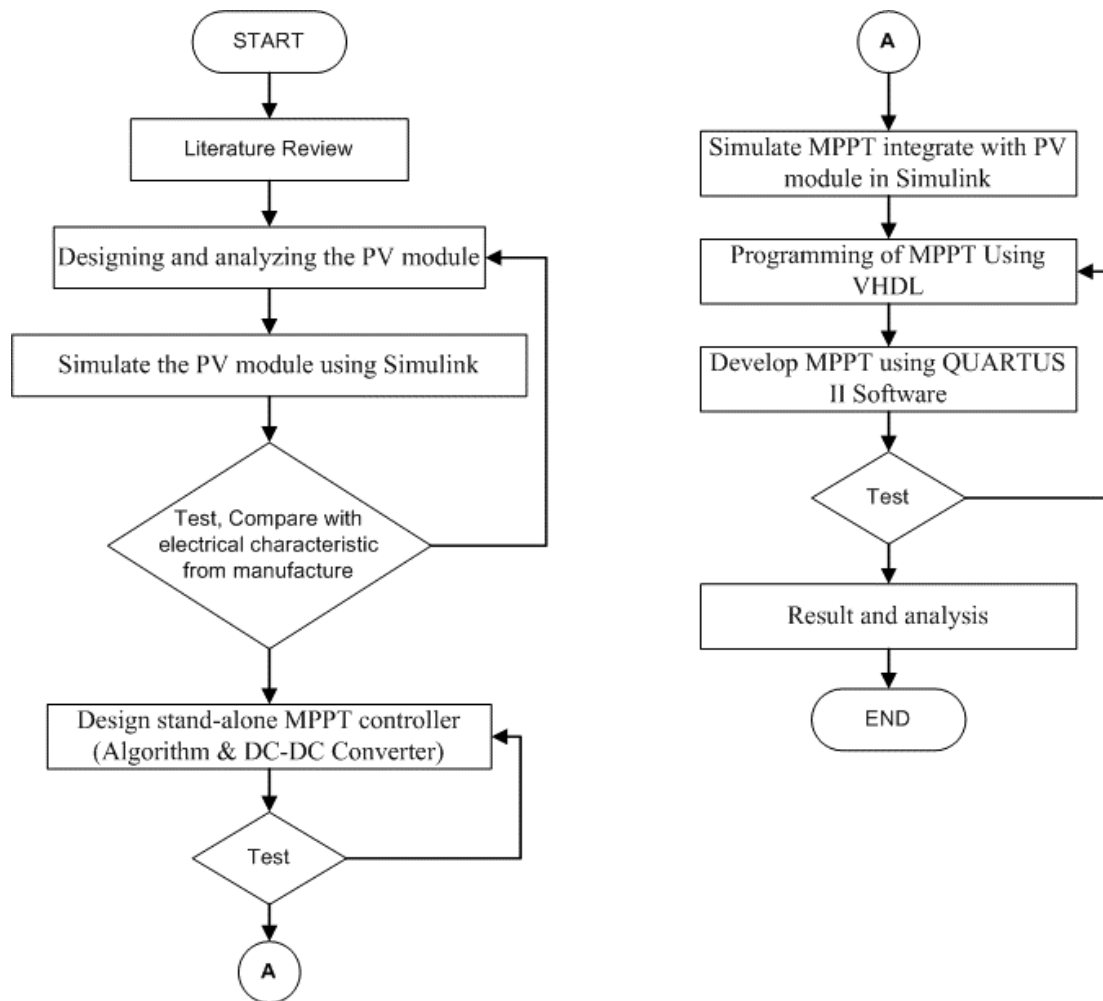


Figure 3.1: Flow chart of project development

### 3.3 Project Development using MATLAB-Simulink

In this section, implementation of MPPT is described in two points of view which are an algorithm of controller and DC-TO-DC converter. In first section, start with a modeling and verification of a photovoltaic module designed in Simulink.

Furthermore, in the next section, discuss on designing the MPPT controller in Simulink. The MPPT algorithm is verified by combined with the DC-TO-DC boost circuit that describe in the last section.

### 3.3.1 Photovoltaic Modeling

PV module will be created by using mathematical modeling of single-diode model. Moreover, the parameter used for PV module is taken from the datasheet of Solar Panel MSX-60.

Furthermore, the mathematical modeling of PV module and MPPT algorithm is applied into Simulink through Embedded S-Function.

#### 3.3.1.1 Mathematical Equation of a Solar Cell

There are many equivalent circuit of a solar cell, where the single-diode and two-diode models could be the most widely used. Since the single model is simple and accurate enough in many case [12], [10], it is applied in this project. The equivalent circuit with series and parallel resistance is shown in Figure 3.2.

The symbols in Figure 3.2 are defined as below:

$I_{ph}$  : Photocurrent;

$I_d$  : Current of parallel diode;

$I_{sh}$  : Shunt current;

$I$  : Output current;

$V$  : Output voltage;

$D$  : Parallel diode;

$R_{sh}$  : Shunt resistance;

$R_s$  : Series resistance;

The  $I - V$  equation of Figure 3.2 is showed as

$$I = I_{ph} - I_0 \left\{ e^{\frac{q(V+R_s I)}{AKT}} - 1 \right\} - \frac{V + R_s I}{R_{sh}} \quad (1)$$

where  $I_0$  is the reverse saturation current of the diode,  $q$  is the electron charge ( $1.602 \times 10^{-19} C$ ),  $A$  is the curve fitting factor, and  $K$  is Boltzmann constant ( $1.38 \times 10^{-23} J / K$ ).

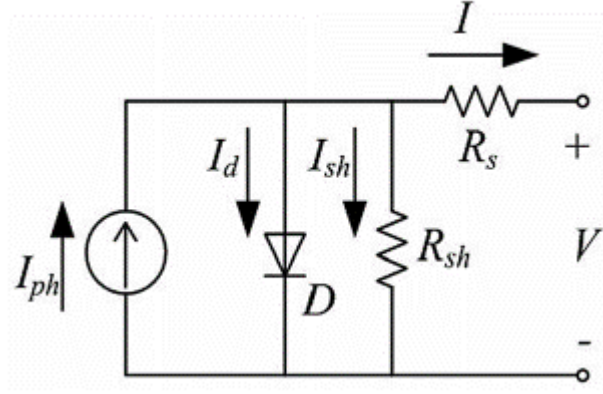


Figure 3.2: Equivalent circuit of a single solar cell

### 3.3.1.2 Model of a PV Module

If a solar cell type tend to have an  $I-V$  curve in which the slope at short circuit is almost zero, the value of  $R_{sh}$  can be assumed to be infinite. In this, the last term in (1) could be ignored. By taking  $I_{ph}$  as  $I_{sc}$ , (1) will become

$$I = I_{sc} - I_0 \left( e^{\frac{q(V+R_s I)}{AKT}} - 1 \right) \quad (2)$$

where  $I_{sc}$  is the short-circuit current.

Equation (2) is valid for a solar cell. For the accurate application of the application of this equation for a PV module, the term of  $q(V+R_s I)/AKT$  is changed to  $q(V+R_s I)/N_s AKT$ , which  $N_s$  is the number of series-connected solar cells in a PV module. Then, (2) will become

$$I = I_{sc} - I_0 \left( e^{\frac{q(V+R_s I)}{N_s AKT}} - 1 \right) \quad (3)$$

A simple PV module model will be derived from (3) in this section. When a PV module is in an open-circuit,  $I = 0$  and the item  $q/N_s AKT$  in (3) will be solved as follows:

$$\frac{q}{N_s AKT} = \frac{\ln \left( \frac{I_{sc}}{I_0} + 1 \right)}{V_{oc}} \quad (4)$$

where  $V_{OC}$  is open-circuit voltage of a PV module.

Substituting (4) into (3), we get

$$I = I_{SC} \left[ 1 - \frac{I_0}{I_{SC}} \left( e^{\ln\left(\frac{I_{SC}+1}{I_0}\right) \frac{(V+R_s I)}{V_{OC}}} - 1 \right) \right] \quad (5)$$

Define  $k = I_{SC} / I_0$  and simplifying (5), to get

$$I = I_{SC} \left[ 1 - \frac{1}{k} (k+1) \frac{V+R_s I}{V_{OC}} + \frac{1}{k} \right] \quad (6)$$

Normally, the value of  $k$  is very large because  $I_0$  is far less than  $I_{SC}$ . Some terms in (6) could be ignored, and then a simple  $I-V$  equation is deduced

$$I = I_{SC} \left( 1 - k \frac{V+R_s I}{V_{OC}} \right) \quad (7)$$

Under standard test condition (STC), which consists of PV module temperature of  $25^\circ C$  and an in-plane irradiance of  $1000W/m^2$  with spectral distribution to an AM1.5 spectrum, (7) could be rewritten as follows:

$$I_{ref} = I_{SC,ref} \left( 1 - k_{ref} \frac{V_{ref} + R_s I_{ref}}{V_{OC,ref}} \right) \quad (8)$$

where  $I_{ref}$  is the output current under STC,  $I_{SC,ref}$  is the short-circuit current under STC,  $V_{ref}$  is the output voltage under STC,  $V_{OC,ref}$  is the open-circuit voltage under STC, and  $k_{ref}$  is the coefficient of  $k$  under STC.

Parameters at maximum output power point (MPP) under STC could be given so solve the coefficient of  $k_{ref}$

$$k_{ref} = \left( \frac{V_{MPP,ref} + R_s I_{MPP,ref}}{V_{OC,ref}} \right) \sqrt{1 - \frac{I_{MPP,ref}}{I_{SC,ref}}} \quad (9)$$

where  $V_{MPP,ref}$  is the output voltage at MPP under STC and  $I_{MPP,ref}$  is the output current at MPP under STC.

## REFERENCES

- [1] R. F. Coelho, F. M. Concer and D. Martins, "A Study of the Basic DC-DC converters," in *10th Brazilian Power Electronics Conference*, 2009.
- [2] R. Faranda and S. Leva, "Energy comparison of MPPT techniques for PV Systems," in *WSWAS Trans. on Power Sys.*, Italy, 2008.
- [3] A. Tariq, J. Asghar and M.S, "Development of microcontroller-based maximum power point tracker for a photovoltaic panel," in *Power India Conference, 2006 IEEE* , New Delhi , 2006.
- [4] S. A. Khan and M. I. Hossain, "Design and Implementation of Microcontroller Based Fuzzy Logic Control for Maximum Power Point Tracking of a Photovoltaic System," in *6th International Conference on Electrical and Computer Engineering*, Dhaka, Bangladesh, 2010.
- [5] C. C. Hua and J. R. Lin, "DSP-Based Controller Application in Battery Storage of Photovoltaic System," in *Industrial Electronics, Control, and Instrumentation, 1996., Proceedings of the 1996 IEEE IECON 22nd International Conference on (Volume:3 )* , 1996.
- [6] D. Das, "FPGA Based Implementation of MPPT of Solar Cell," in *National Conference on Computing and Communication Systems (NCCCS)*, 2012.
- [7] A. Messai and et al., "Maximum power point tracking using a GA optimized fuzzy logic controller and its FPGA implementation," in *Solar energy*, 2011.
- [8] R. F. Coelho and D. C. Martins, "An Optimized Maximum Power Point Tracking Method," *InTech*, pp. 89-113, 2012.
- [9] A. Ahmed and EL TAYYAN, "A simple method to extract the parameters of the single-diode model of a PV," *Turkish Journal of Physics*, pp. 121-131, March 2013.
- [10] W. Kim and W. Choi, "A novel parameter extraction method for the one-diode

- solar cell model," *Solar Energy*, Vols. 84, no.6, pp. 1008-1019, Jun. 2010.
- [11] B. Liu, S. Duan, F. Liu and P. Xu, "Analysis and Improvement of Maximum Power Point Tracking Algorithm Based on Incremental Conductance Method for Photovoltaic Array," in *PEDS*, 2007.
- [12] W. D. Soto, S. A. Klein and W. A. Beckman, "Improment and validation of a model for photovoltaic array performance," *Solar Energy*, Vols. 80, no.1, pp. 78-88, Jan. 2006.
- [13] W. Herrmann and W. Wiesner, "Current-voltage translation procedure for PV generators in German 1000 roofs-programme," in *EUROSUN Conf.*, Freiburg, German, 1996.
- [14] E. Matagne, R. Chenni and R. E. Bachtiri, "A photovoltaic cell model based on nominal data only," in *Proc. Int. Conf. Power Eng., Energy Electr. Drives*, 2007.
- [15] K. Ding, X. Bian, H. Liu and T. Peng, "A MATLAB-Simulink-Based PV Module Model and Its Application Under Conditions of Nonuniform Irradiance," *IEEE Trans. on Energy Convers.*, Vols. 27, no.4, pp. 864-872, Dec. 2012.
- [16] C. S. Chin, P. Neelakantan, H. P. Yoong and K. T. Teo, "Control and optimization of fuzzy based maximum power point tracking in solar photovoltaic system," in *Global Conference on Power Control and*, 2010.
- [17] S. Brown and Z. Vranesic, *Fundamentals of Digital Logic with VHDL Design*, 2nd ed., New York: McGraw Hill, 2005.
- [18] J. Zhang and F. Guo, "The Study in Photovoltaic Control System Based on FPGA," in *Research Challenges in Computer Science, 2009. ICRCCS '09*, Shanghai , 2009.
- [19] C. C. Hua and C. M. Shen, "Control of DC/DC converters for solar energy system with maximum power tracking," in *Industrial Electronics, Control and Instrumentation, 1997. IECON 97. 23rd*, New Orleans, LA , 1997.
- [20] W. Kim and W. Choi, "A novel parameter extraction method for the one-diode solar cell model," in *Solar Energy*, Jun. 2010.
- [21] Z. Cheng, H. Yang and Y. Sun, "FPGA-based PV systems fuzzy MPPT control algorithm," in *2010 Seventh International Conference on Fuzzy Systems and Knowledge Discovery (FSKD 2010)*, 2010.